



Comparison of the distribution of the Bartholin and/or Rivinus salivary ducts assessed with magnetic resonance-sialography in patients with ranula and in healthy subjects

Nao Wakasugi-Sato¹, Tatsuro Tanaka², Masafumi Oda¹, Shinobu Matsumoto-Takeda¹, Manabu Habu³, Shun Nishimura¹, Osamu Takahashi³, Ikuko Nishida⁴, Hiroki Tsurushima⁵, Taishi Otani⁵, Jumpei Tanaka⁵, Susumu Nishina¹, Daigo Yoshiga⁵, Masaaki Sasaguri³, Yasuhiro Morimoto¹

¹Division of Oral and Maxillofacial Radiology, Kyushu Dental University, Kitakyushu, Japan; ²Department of Maxillofacial Radiology, Graduate School of Medical and Dental Sciences, Kagoshima University, Kagoshima, Japan; ³Division of Maxillofacial Surgery, Kyushu Dental University, Kitakyushu, Japan; ⁴Division of Developmental Stomatognathic Function Science, Kyushu Dental University, Kitakyushu, Japan; ⁵Division of Oral Medicine, Kyushu Dental University, Kitakyushu, Japan

Contributions: (I) Conception and design: N Wakasugi-Sato, Y Morimoto; (II) Administrative support: S Matsumoto-Takeda, I Nishida, S Nishina; (III) Provision of study materials or patients: M Habu, O Takahashi, H Tsurushima, T Otani, J Tanaka, D Yoshiga, M Sasaguri; (IV) Collection and assembly of data: N Wakasugi-Sato, M Oda, S Nishimura; (V) Data analysis and interpretation: N Wakasugi-Sato, T Tanaka, M Oda, Y Morimoto; (VI) Manuscript writing: All authors; (VII) Final approval of manuscript: All authors.

Correspondence to: Yasuhiro Morimoto, DDS, PhD. Division of Oral and Maxillofacial Radiology, Kyushu Dental University, 2-6-1 Manazuru, Kokurakita-ku, Kitakyushu 803-8580, Japan. Email: rad-mori@kyu-dent.ac.jp.

Background: The distribution and drainage of the sublingual gland ducts have various patterns that might be related to sublingual gland-related diseases, including ranula. This study aimed to elucidate the characteristics of the distribution of Bartholin and/or Rivinus ducts in patients with ranula using magnetic resonance (MR) sialography.

Methods: In this retrospective cross-sectional study, the distributions and drainage patterns of sublingual gland ducts on MR sialography were classified in 74 subjects without sublingual gland-related disease as confirmed by both medical history and clinical examination and 15 patients with ranula, respectively. All patients had visited Kyushu Dental University Hospital from July 2015 to June 2022 to undergo MR imaging. Data on the distributions and drainage patterns of the sublingual gland ducts, including the characteristics of the Bartholin and/or Rivinus ducts, were then statistically compared between subjects without sublingual gland-related disease and patients with ranula. The images were assessed by an experienced oral and maxillofacial radiology specialist certified by the Japanese Society for Oral and Maxillofacial Radiology. The distributions (five groups) and drainage patterns (three patterns) of the sublingual gland ducts on MR sialography were classified in reference to previous studies, with some modifications in all subjects without sublingual gland-related disease and patients with ranula.

Results: A significant difference in the distribution of the ducts ($P < 0.001$), with a low number of patients exposing an undetected canal or Rivinus duct, was found in the group of patients with ranula ($P < 0.05$). Regarding drainage patterns, no patient with ranula presented a Rivinus duct only. A significant difference in the drainage patterns of the sublingual gland ducts on MR sialography was observed between subjects without sublingual gland-related disease and patients with ranula ($P = 0.001$).

Conclusions: The present results suggest that the distribution of the sublingual gland ducts, mainly, the Bartholin duct, may be related to ranula formation. These findings also demonstrate that MR sialography contributes well to preoperative evaluation and is effective for assessing the complex excretory distribution of the sublingual gland ducts.

Keywords: Magnetic resonance sialography (MR sialography); ranula; sublingual gland ducts; classification

Submitted Jun 29, 2023. Accepted for publication Oct 16, 2023. Published online Nov 09, 2023.

doi: 10.21037/qims-23-948

View this article at: <https://dx.doi.org/10.21037/qims-23-948>

Introduction

Together with the parotid and submandibular glands, the sublingual gland is one of the three major salivary glands. The parotid gland secretes serous saliva, whereas the submandibular and sublingual glands secrete a mixture of serous and mucous saliva (1). The sublingual glands are located in pairs in the submucosa of the lingual floor of the oral cavity on both sides of the mandible (2). They are elongated anteriorly and posteriorly, measure about 2.5 cm, and are shaped like flattened almonds (3). The long, thick conduits of the sublingual gland are called Bartholin ducts, and the many smaller, independently opening conduits are called Rivinus ducts (1). Both types of ducts open into the sublingual folds of the oral floor mucosa (1). The salivary glands secrete saliva containing enzymes to digest food in one lump, which is excreted into the oral cavity through the salivary gland ducts.

Excretion of a saliva excreted from the sublingual glands can be impaired for various reasons, including injury to the sublingual gland ducts, and the resulting retention cyst is called a ranula. When confined to the sublingual gland, it is referred to as a simple ranula, and when extending to the submandibular space, it is referred to as a plunging ranula. As it is a relatively common mucosal disease of the floor of the oral cavity (3), it is important to clarify the cause of ranula for appropriate diagnosis and treatment, including surgical procedures.

Unlike X-ray sialography, magnetic resonance (MR) sialography is noninvasive and does not require cannulation of the duct, injection of contrast medium, or the use of ionizing radiation to examine salivary gland ducts (4). MR sialography has shown high diagnostic potentialities, and has been effectively introduced in clinical practice, similar to MR cholangiopancreatography (MRCP) (4). In a recent study, we reported that MR sialography is a useful technique for the clinical evaluation of sublingual gland ducts in addition to parotid and submandibular glands (5-9). MR sialography can visualize very thin and very short sublingual gland ducts that have a diameter and length of only 1 mm (5). Images of sublingual glands and sublingual gland

ducts on MR sialography are identical to those seen in an oral anatomy textbook (2). In a previous study involving subjects without sublingual gland-related disease, we noticed different distributions of Bartholin and/or Rivinus ducts and different drainage patterns in sublingual gland ducts on MR sialography. However, we could not precisely report the distribution of Bartholin and/or Rivinus ducts or the anatomical drainage patterns in sublingual gland ducts on MR sialography because of our focus on the clinical applications of dynamic MR sialography (5).

We hypothesized that visualization of sublingual gland ducts could indicate the clinical significance of sublingual gland-related diseases, including ranula. Because ranulas are derived from sublingual gland ducts, the distribution of Bartholin and/or Rivinus ducts, and in particular, the presence of the Bartholin duct, may be related to ranula formation (10). By contrast, other investigations have indicated that Rivinus ducts are always present and involved in the formation of ranulas through a tear (11,12). No definite hypothesis has been established. Given this background, the purpose of this study was to investigate whether the distribution of the Bartholin and Rivinus ducts, conduits of the sublingual gland, and their drainage patterns are involved in the pathogenesis of ranula. To this end, the distribution of Bartholin and Rivinus ducts and their drainage patterns were classified on MR sialography and compared between subjects without sublingual gland-related disease and patients with ranula. We present this article in accordance with the STROBE reporting checklist (available at <https://qims.amegroups.com/article/view/10.21037/qims-23-948/rc>).

Methods

A total of 74 subjects without sublingual gland-related disease (26 men and 48 women; mean age, 57.4 years; age range, 14–85 years), as verified by both medical history and clinical examination, were retrospectively and cross-sectionally investigated, as were 15 consecutive patients with ranula (13 sublingual, 2 plunging; 3 men, 12 women; mean age, 34.5 years; age range, 6–92 years). All patients

Table 1 Distribution of subjects without sublingual gland-related disease and patients with ranula

Variables	Subjects		Ranulas	
	Men	Women	Men	Women
Number	26	48	3	12 [#]
Age (years)				
Mean ± SD	56.1±18.5	59.9±18.0	47.3±39.0	31.2±19.5
Range	16–84	14–85	20–92	6–68

[#], only one of the ranula was analyzed microscopically after surgical procedure; ^{*}, two patients had plunging ranula. SD, standard deviation.

had visited Kyushu Dental University Hospital from July 2015 to June 2022 to undergo magnetic resonance imaging (MRI). Data from the subjects without sublingual gland-related disease and patients with ranula are shown in *Table 1*. Images of 74 subjects without sublingual gland-related disease were selected from the hospital database of patients who had undergone MR sialography of the sublingual gland (*Figure 1*). Of the 4,384 patients who underwent MRI at Kyushu Dental University Hospital, 134 patients underwent MR sialography. Among these 134, 45 patients were excluded as follows: seven patients who did not undergo MRI for the first time, 14 patients who were not evaluated due to artifacts, 21 who underwent MR sialography only on the lesion side (9 patients with carcinoma, 1 with pleomorphic adenoma, 2 mucocele, 2 with sublingual adenitis, 6 with submandibular adenitis, and 1 with cellulitis), and 3 with Sjögren syndrome. Finally, 74 subjects without sublingual gland-related disease and 15 patients with ranula were analyzed (*Figure 1*). We used images that included the sublingual gland area when sialography was taken for the submandibular and parotid glands, as well as images of the contralateral side that were unrelated to the main complaint. Only one image was analyzed microscopically after surgery. In the rest of the cases, there was no histological confirmation, only a clinical diagnosis.

An image of a single side (randomly chosen) or a disease-related side of the sublingual gland ducts was used because only single images could be acquired. As mentioned above, images of the non-primary side or of MR sialography for the submandibular gland that depicted the sublingual gland portion were used for 74 subjects. Therefore, we thought it more appropriate to use one side for each subject. For the MRI examinations, informed consent was obtained from all patients or their parents/legal guardians. Individual consent

for this retrospective analysis was waived. All patient rights were protected by the Human Investigations Committee of Kyushu Dental University. This study was approved by the institutional review board of Kyushu Dental University (No. 20-27). The study was conducted in accordance with the Declaration of Helsinki (as revised in 2013).

All images were acquired using a 1.5-T full-body MR system (EXCELART Vantage powered by Atlas; Toshiba, Tokyo, Japan) with a head coil (Atlas Head SPEEDER) to visualize the sublingual gland ducts with reference to Tanaka *et al.* (5) and Oda *et al.* (13). T1-weighted, short-tau inversion recovery, and three-dimension fast asymmetric spin-echo (3D-FASE) images were acquired for each subject. The imaging parameters used in these sequences are shown in *Table 2*.

3D-MR sialography for the sublingual gland ducts was acquired according to Tanaka *et al.* (5) (*Table 2*). MR sialography was performed using 3D-FASE sequencing for the same session in which conventional MR studies of the sublingual glands were obtained. After a single excitation, images were acquired using MR sequences (shown in *Table 2*) with fat saturation to suppress the signals from the subcutaneous fat. The imaging volume was centered parasagittally for the midline of the sublingual gland. As post-processing of the MR sialographic images, the maximum intensity projection reconstructions were used for all subjects without sublingual gland-related disease and patients with ranula. Using 3D acquisition, any required orientation can be reformatted. The sublingual gland ducts were identified on an initial set of axial 3D-FASE images. The imaging time required for MR sialographic 3D-reconstruction images using 3D-FASE sequencing was 6 minutes 30 seconds. A sialogogue was not used in the 3D-MR sialography for the sublingual gland duct.

The images were assessed by an experienced (14 years) oral and maxillofacial radiologist (Wakasugi-Sato N) who is a specialist certified by the Japanese Society for Oral and Maxillofacial Radiology. The distributions (five groups) and drainage patterns (three patterns) of the sublingual gland ducts on MR sialography were classified in reference to Zhang *et al.* (14) and Mun *et al.* (10), with some modifications, as described below, in all subjects without sublingual gland-related disease and patients with ranula.

- ❖ Group 0: unable to detect the sublingual gland ducts;
- ❖ Group 1 (= Pattern 1): Rivinus ducts only (*Figure 2A*);
- ❖ Group 2: Bartholin duct only (*Figure 2B*);
- ❖ Group 3: Rivinus ducts and Bartholin duct, but

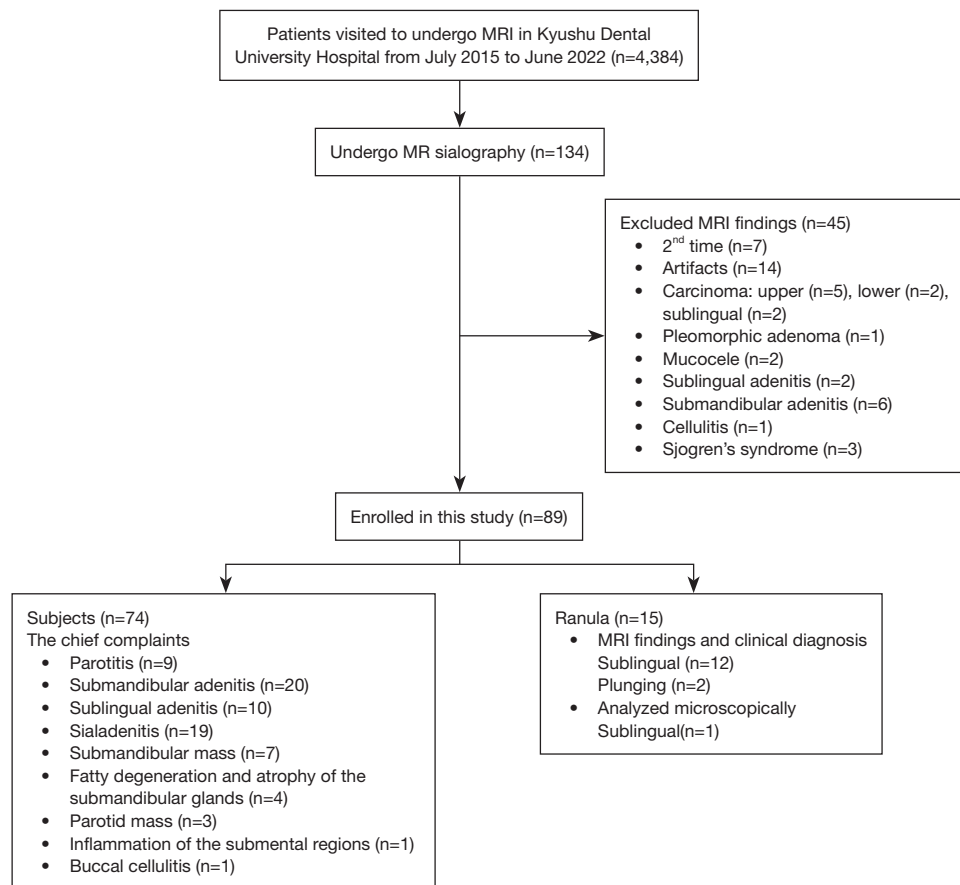


Figure 1 Flow chart showing the recruitment of the participants, from the initial selection of potentially eligible patients to the final inclusion of patients, with reasons for any exclusion. Of the 4,384 patients who underwent MRI at Kyushu Dental University Hospital, 134 underwent MR sialography, 45 of whom were excluded as follows: seven patients who did not undergo MRI for the first time, 14 who were not evaluated due to artifacts, 21 who underwent MR sialography only on the lesion side (nine patients with carcinoma, one with pleomorphic adenoma, two mucoceles, two with sublingual adenitis, six with submandibular adenitis, and one with cellulitis), and three patients with Sjögren syndrome. Finally, 74 subjects without sublingual gland-related disease and 15 patients with ranula were analyzed. MRI, magnetic resonance imaging.

Table 2 Imaging parameters of each sequence

Imaging parameters	Sequences		
	STIR	T1WI	3D-FASE
TR (ms)	4,700	805	6,000
TE (ms)	75	10	250
Flip angle (°)	90	90	90
FOV (mm)	200×200	200×200	200×200
Section thickness (mm)	6	6	1.8
Matrix (pixels)	272×272	224×320	320×320
Acquisition time (min:s)	4:38	2:04	6:30

STIR, short T1 inversion recovery; T1WI, T1-weighted image; 3D-FASE, three-dimension fast asymmetric spin-echo; TR, repetition time; TE, echo time; FOV, field of view.

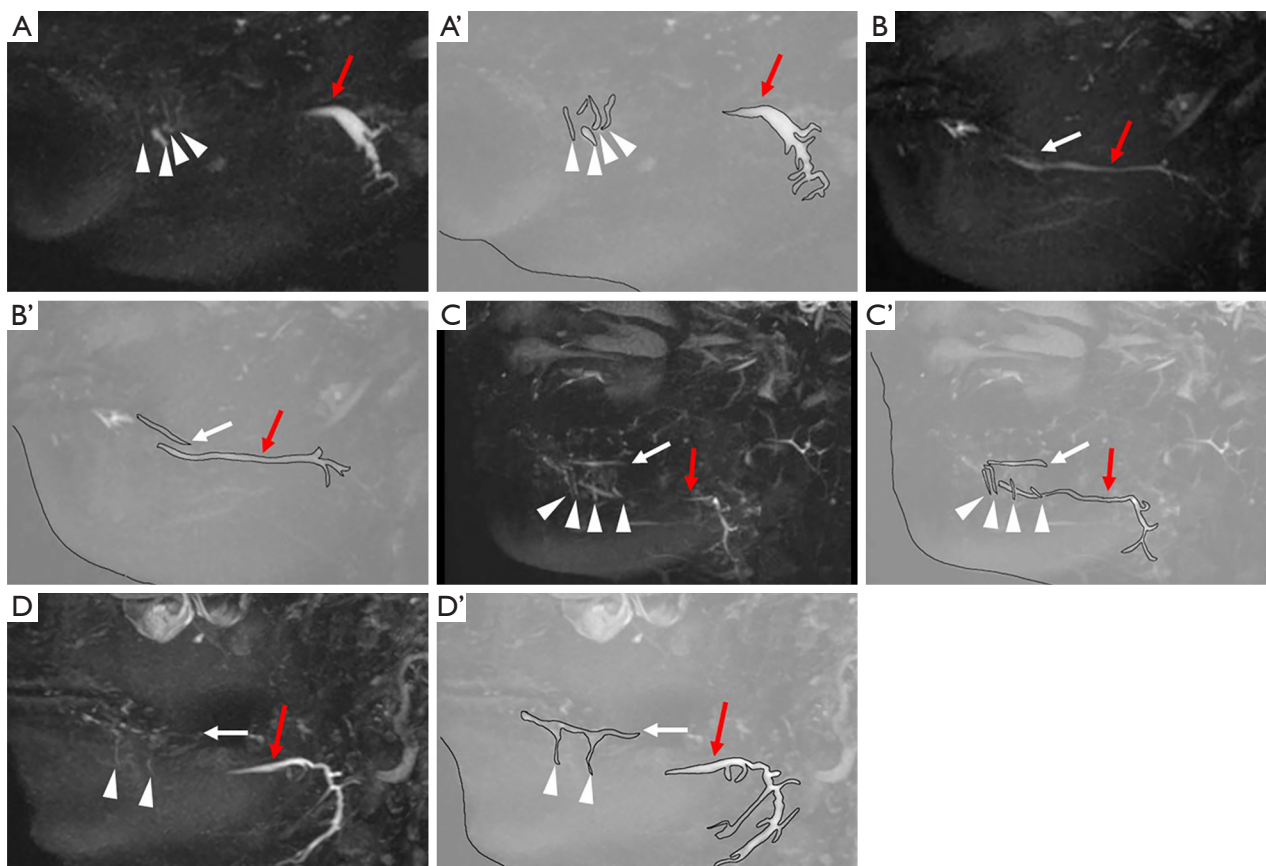


Figure 2 Distribution of the Bartholin and/or Rivinus ducts in subjects without sublingual gland-related disease on MR sialography. (A) Group 1: only the Rivinus ducts (arrowheads) were visualized in the sublingual glands. Extraglandular portions of the typical Rivinus ducts (arrowheads) could be identified as a few bright homogeneous ascending linear structures in continuity from the sublingual glands. The Wharton duct (red arrow) can be seen on the right edge. (A') Schema of (A): only the Rivinus ducts (arrowheads) were visualized in the sublingual glands. The Wharton duct can be seen on the right edge (red arrow) as one bright homogeneous linear structure. (B) Group 2: only the Bartholin duct (white arrow) was visualized in the sublingual glands. Extraglandular portions of the typical Bartholin duct (white arrow) could be identified as one bright homogeneous linear structure. The Wharton duct (red arrow) can be seen as one bright homogeneous linear structure under the Bartholin duct. (B') Schema of (B): only the Bartholin duct (white arrow) was visualized in the sublingual glands. The Wharton duct (red arrow) can be seen as one bright homogeneous linear structure under the Bartholin duct. (C) Group 3: the Bartholin duct (white arrow) as one bright homogeneous linear structure and the Rivinus ducts (arrowheads) as a few bright homogeneous ascending linear structures were visualized in the sublingual glands, but both ducts were separated. The Wharton duct (red arrows) can be seen as one bright homogeneous linear structure across the Rivinus ducts (arrowheads) and under the Bartholin duct (white arrow). (C') Schema of (C): the Bartholin duct (white arrow) as one bright homogeneous linear structure and the Rivinus ducts (arrowheads) as a few bright homogeneous ascending linear structures were visualized in the sublingual glands, but both ducts were separated. The Wharton duct (red arrows) can be seen as one bright homogeneous linear structure across the Rivinus ducts (arrowheads) and under the Bartholin duct (white arrow). (D) Group 4: the Bartholin duct (white arrow) as one bright homogeneous linear structure and the Rivinus ducts (arrowhead) as bright homogeneous ascending linear structures were visualized in the sublingual glands, and both ducts were fused. The Wharton duct (red arrow) can be seen on the right edge (red arrow). (D') Schema of (D): the Bartholin duct as one bright homogeneous linear structure (white arrow) and the Rivinus ducts as bright homogeneous ascending linear structures (arrowhead) were visualized in the sublingual glands, and both ducts were fused. The Wharton duct (red arrow) can be seen on the right edge. MR, magnetic resonance.

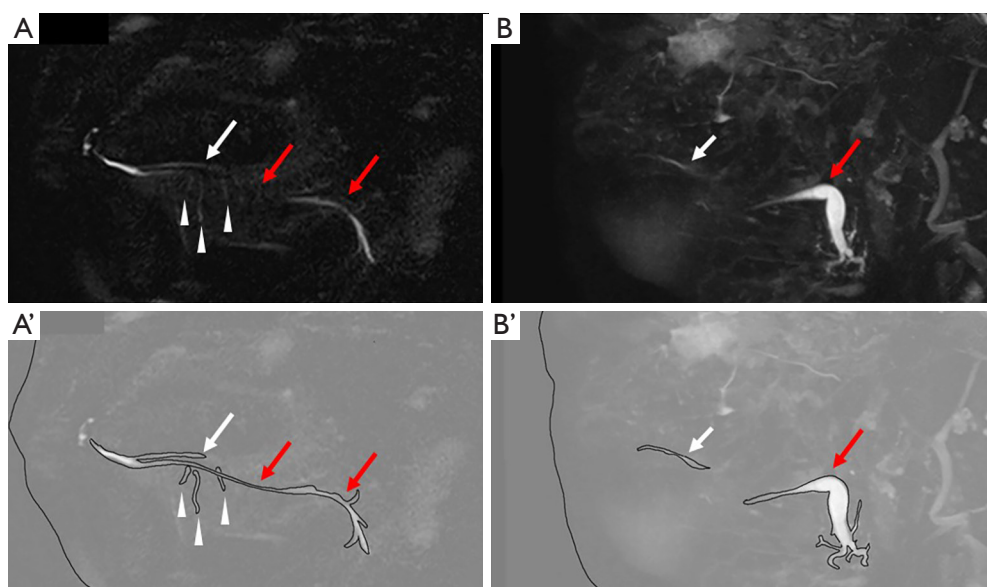


Figure 3 Drainage patterns of the Bartholin and/or Rivinus ducts in subjects without sublingual gland-related disease on MR sialography. (A) Drainage of the Rivinus ducts (arrowheads) as a few bright homogeneous ascending linear structures and the Bartholin duct (white arrow) as one bright homogeneous linear structure into the Wharton duct (red arrows) were visualized in the sublingual glands. (A') Schema of (A): the Rivinus ducts (arrowheads) as a few bright homogeneous ascending linear structures and the Bartholin duct (white arrow) as one bright homogeneous linear structure into the Wharton duct (red arrows) were visualized in the sublingual glands. (B) Drainage of the Bartholin duct (white arrow) as one bright homogeneous linear structure into the oral floor was visualized in the sublingual glands. The Wharton duct (red arrow) can be seen on the right edge. (B') Schema of (B): the Bartholin duct (white arrow) as one bright homogeneous linear structure into the oral floor was visualized in the sublingual glands. The Wharton duct (red arrow) can be seen on the right edge. MR, magnetic resonance.

both were separated (*Figure 2C*);

- ❖ Group 4: Rivinus ducts and Bartholin duct, but both were fused (*Figure 2D*).

Drainage patterns were classified in relation to the sublingual gland ducts and Wharton duct. The classification was based on the number of people, excluding Group 0.

- ❖ Pattern 1: Rivinus ducts only;
- ❖ Pattern 2: Bartholin duct into the Wharton duct (*Figure 3A*);
- ❖ Pattern 3: Bartholin duct into the oral floor (*Figure 3B*).

The numbers of Rivinus and Bartholin ducts into the Wharton duct (Pattern 2; *Figure 3A*) or of the Bartholin duct into the oral floor (Pattern 3; *Figure 3B*) were also evaluated.

All statistical analyses were performed using SPSS version 11 (SPSS, Chicago, IL, USA). Categorical variables were compared using a two-sided χ^2 test. Residual analysis was used to identify which items were significantly different between the two groups. Fisher's exact test was used to test

for differences in ranula development by gender. The *t*-test was used to test for age differences. Values of $P < 0.05$ were considered to indicate statistical significance.

Results

Identification and distribution of the Bartholin and/or Rivinus ducts on MR sialography in subjects without sublingual gland-related disease

The chief complaints of the 74 subjects without sublingual gland-related disease who underwent MR sialography were parotitis in nine, submandibular adenitis in 20, sublingual adenitis in 10, sialadenitis in 19, submandibular mass in seven, fatty degeneration and atrophy of the submandibular glands in four, parotid mass in three, inflammation of the submental regions in one, and buccal cellulitis in one (*Figure 1* and *Table 1*). The chief complaint of all 15 patients with ranula was swelling of the sublingual or submandibular area (*Figure 1* and *Table 1*). Three of these patients also

Table 3 Distribution of sublingual gland ducts in subjects without sublingual gland-related disease and patients with ranula

Groups	Subjects		Ranulas	
	Numbers	%	Numbers	%
0	24	32.4	1*	6.7
1	22	29.7	0*	0
2	4	5.4	3	20.0
3	22	29.7	6	40.0
4	2*	2.7	5	33.3

*, significantly smaller in residual analysis $P < 0.05$. Group 0: unable to detect ducts; Group 1: ducts of Rivinus only; Group 2: duct of Bartholin only; Group 3: Bartholin and Rivinus ducts, but both were separated; Group 4: Bartholin and Rivinus ducts, but both were fused.

Table 4 Distribution of drainage patterns in subjects without sublingual gland-related disease and patients with ranula

Patterns	Subjects		Ranulas	
	Numbers	%	Numbers	%
1	22	44	0*	0
2	23	46	8	57.1
3	5*	10	6	42.9

*, significantly smaller in residual analysis $P < 0.05$. Pattern 1: ducts of Rivinus only; Pattern 2: duct of Bartholin into the Wharton duct; Pattern 3: duct of Bartholin into the oral floor.

complained of recurrent swelling and healing. No significant gender differences were found between subjects and patients with ranula (Fisher's exact test, $P = 0.368$) (Table 1). Patients with ranula were significantly younger than the healthy subjects (t -test, $P < 0.001$) (Table 1).

Rivinus ducts could be identified as a few high-signal linear structures ascending from the sublingual glands on MR sialography (Figure 2A). The duct of Bartholin was identified as a linear line with high-signal traversing within the sublingual glands on MR sialography (Figure 2B). The distributions of Bartholin and/or Rivinus ducts of the sublingual glands in subjects without sublingual gland-related disease on MR sialography are shown in Table 3. Rivinus and Bartholin ducts were not visualized in 32.4% of the subjects without sublingual gland-related disease (Group 0). Rivinus ducts were visualized only as a distribution of sublingual gland ducts in 29.7% of the subjects without sublingual gland-related disease (Group 1). In Group 1, the number

of Rivinus ducts was 4.0 ± 1.63 [mean \pm standard deviation (SD)], while the Bartholin duct was only visualized in 5.4% (Group 2). The Bartholin and Rivinus ducts were fused and separate in 29.7% (Group 3) and 2.7% (Group 4) of the subjects without sublingual gland-related disease, respectively. In Group 3, the number of Rivinus ducts was 4.5 ± 2.26 (mean \pm SD).

The drainage patterns of the sublingual gland ducts using MR sialography are shown in Table 4. In 44% of the subjects without sublingual gland-related disease, drainage of the sublingual gland ducts was only seen in the Rivinus ducts (Pattern 1). In 46% of the subjects without sublingual gland-related disease, drainage of the Bartholin duct into the Wharton duct was seen (Pattern 2), and in 10% of the subjects without sublingual gland-related disease, drainage from the Bartholin duct into the oral floor was observed (Pattern 3).

Distributions of the Bartholin and/or Rivinus ducts on MR sialography in patients with ranula

The distributions of Bartholin and/or Rivinus ducts in patients with ranula on MR sialography are shown in Table 3. There were no ranula patients, with only the Rivinus ducts visualized (Group 1). In 20% of the patients, only the Bartholin duct was visualized (Group 2; Figure 4A). In 40% and 33.3% of the patients, the Bartholin and/or Rivinus ducts were separated (Group 3; Figure 4B) and fused (Group 4; Figure 4C), respectively.

The drainage patterns of sublingual gland ducts on MR sialography are shown in Table 4. In 57.1% of the patients, drainage of the Bartholin duct into the Wharton duct was seen (Pattern 2; Figure 4B). In 42.9% of the patients, drainage from the Bartholin duct into the oral floor was observed (Pattern 3; Figure 4A).

Difference in the distribution of the Bartholin and/or Rivinus ducts on MR sialography between subjects without sublingual gland-related disease and patients with ranula

A significant difference in the distribution of Bartholin and/or Rivinus ducts on MR sialography was found between subjects without sublingual gland-related disease and patients with ranula (Table 3; $P < 0.001$, two-sided χ^2 test). The majority of Bartholin and/or Rivinus ducts in subjects without sublingual gland-related disease was seen in Group 1, i.e., only the Rivinus ducts could be detected by residual analysis, whereas in patients with ranula, the

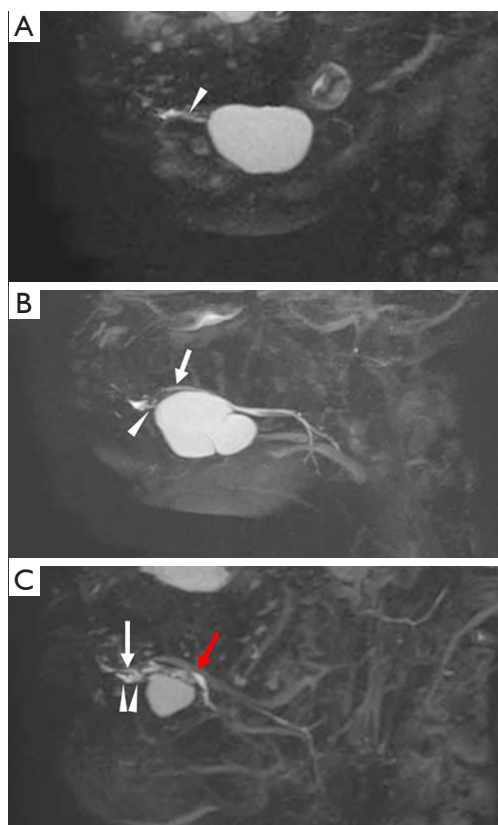


Figure 4 Distribution and drainage patterns of the Bartholin and/or Rivinus ducts in patients with ranula on MR sialography. (A) Only the Bartholin duct as one bright homogeneous linear structure (arrowhead) was visualized adjacent to the ranula. (B) The Rivinus ducts as bright homogeneous linear structures (arrowhead) and the Bartholin duct as one bright homogeneous linear structure (white arrow) into the oral floor adjacent to the ranula were visualized in the sublingual glands. (C) The Rivinus ducts as a few bright homogeneous ascending linear structures (arrowhead) and the Bartholin duct as one bright homogeneous linear structure (white arrow) into the Wharton duct (red arrow) adjacent to the ranula was fused in the sublingual glands (arrowhead). MR, magnetic resonance.

Bartholin and Rivinus ducts could significantly both be detected significantly by residual analysis ($P < 0.05$). By contrast, only the Rivinus ducts (Group 1) could not be detected in patients with ranula. In addition, a significant difference in the drainage patterns of the sublingual gland ducts on MR sialography was observed between subjects without sublingual gland-related disease and patients with ranula (Table 4; $P = 0.001$, two-sided χ^2 test). The drainage of the sublingual gland ducts was only seen significantly

in the Rivinus ducts in about 44% of the subjects without sublingual gland-related disease by residual analysis ($P < 0.05$) (Pattern 1). This result suggests that the distribution of the sublingual gland ducts, mainly, the Bartholin duct may be related to ranula formation.

Discussion

In a recent study, we demonstrated for the first time the imaging characteristics of the sublingual gland ducts obtained on MR sialography, such as ascending Rivinus ducts with a diameter and length of less than 1 mm, as shown in anatomy textbooks (2,5). In the present study, we analyzed the distribution and drainage patterns of the Bartholin and/or Rivinus ducts using MR sialography to elucidate the relationship between the Bartholin duct and the occurrence of ranulas based on a comparison between subjects without sublingual gland-related disease and patients with ranula.

The most interesting result of the present study is that there were significant differences in the distribution of these ducts and drainage patterns on MR sialography. There was no distribution pattern of only Rivinus ducts (Group 1 and Pattern 1) in patients with ranula. In addition, the Bartholin duct was found more frequently in the sublingual glands in patients with ranula than in subjects without sublingual gland-related disease. This result suggests that the distribution of the sublingual gland ducts, mainly, the Bartholin duct may be related to ranula formation.

The etiology of ranula could not be clearly identified, but inflammation or trauma is typically considered (3). Injury to the oral floor caused by inflammation or trauma can induce obstruction of the sublingual gland ducts, leading to ranula (3). The obstruction of the sublingual gland ducts after injury to the oral floor may be related to the Bartholin and/or Rivinus ducts.

Consequently, the occurrence of ranula should be related to the Bartholin duct, which has a single aperture, but not to Rivinus ducts, which have multiple apertures. A previous report suggested that the presence of the Bartholin duct may be related to ranula formation, as demonstrated by surgical findings regarding sublingual gland ducts in patients with ranula (10). Anatomic variation in Bartholin and Wharton ducts is common in patients with ranula, and no variation in the Bartholin duct has been identified in patients without ranula during surgical procedures (10). The present results also support the opinion that the presence of the Bartholin duct may be related to ranula formation. More participants

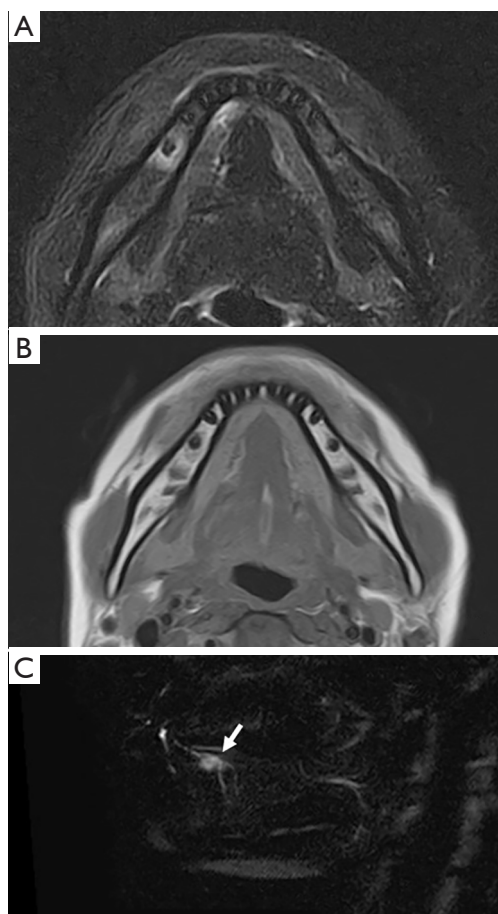


Figure 5 Identification of ranula derived from the Bartholin duct in patients with ranula on MR sialography. STIR (A), T1-weighted images (B), and MR sialography (C) in a 15-year-old woman with ranula in the right oral floor. A mass lesion is seen in continuity with the sublingual glands on STIR (A) and T1-weighted images (B), and was diagnosed as ranula. The mass is derived from the Bartholin duct as one bright homogeneous linear structure (arrow) (C). MR, magnetic resonance; STIR, short-tau inversion recovery.

were included in the present study compared with previous studies because the procedure was MRI as opposed to surgery. Therefore, we recommend that MR sialography be used for the evaluation of suspected ranula. However, the obscuring of one part of the Bartholin and/or Rivinus ducts was seen in patients with ranula on MR sialography. Other investigations have reported that Rivinus ducts were always present and involved in the formation of ranula through a tear (11,12). Leppi examined both sides of eight autopsies and 20 cadavers (11) and reported that a lesser sublingual gland was always present and consisted of a mass of small

glands, from each of which a short Rivinus duct passed to the plica sublingualis (11). McGurk *et al.* (12) histologically examined eight ranulas with the associated sublingual gland and in every case, found communication between the sublingual gland and ranula via a torn Rivinus duct. Rupture of one of the Rivinus ducts can result in the extravasation of saliva into the surrounding tissues to form an extravasation cyst or ranula (15). In the present study, we did not exclude the possibility that the Rivinus ducts are involved in the pathogenesis of ranula, as previous studies have pointed out. However, in this study, the patients with ranula had few Rivinus ducts at a level that could be observed on MR sialography. Care should be taken when evaluating the relationship between the origin of ranula and the distribution of the sublingual gland ducts (Figure 5). In the future, we would like to elucidate the clinical significance of MR sialography of the sublingual gland ducts by its clinical applications for many kinds of diseases on the oral floor, including sublingual gland-related diseases.

The other interesting result of the present study is that the distribution and drainage patterns of the Bartholin and/or Rivinus ducts on MR sialography were classified in subjects without sublingual gland-related disease. In 5.4% of the subjects without sublingual gland-related disease, only the Bartholin duct was visualized on MR sialography. In addition, both the Bartholin and Rivinus ducts were visualized in 29.7% of the subjects without sublingual gland-related disease, whereas the Rivinus ducts were visualized as a distribution of the sublingual gland ducts in 29.7%. Regarding the drainage patterns of the sublingual gland ducts, the Bartholin duct drained into the Wharton duct in 46% of the subjects without sublingual gland-related disease, whereas drainage of the sublingual gland ducts was only seen in the Rivinus ducts in 44%. Finally, in 10% of the subjects without sublingual gland-related disease, drainage from the Bartholin duct into the oral floor was observed. MR sialography was able to detect the precise running of Bartholin and/or Rivinus ducts, and our data indicated that the distribution and drainage patterns were one of the criteria. The distribution of the Bartholin and Rivinus ducts in the present study did not differ much from that in cadavers, as reported by Leppi (11). However, the number of Rivinus ducts varied from 8 to 30, which differed from the results reported by Leppi (11). It is possible that part of the Rivinus ducts could not be detected because very thin and short ducts with a diameter and length of only 1 mm, such as those shown in anatomy textbooks, are difficult to visualize (2). In addition, in many cases, it

is difficult to distinguish between vessels and Wharton's canal because of the complex anatomy of the same region on MR sialography. One possible explanation for this is the difference between the use of MR sialography for active subjects and autopsies for cadavers. In the future, we would like to clarify the actual situation through a comparative study of the distribution of the Bartholin and Rivinus ducts in surgical cases involving ranula and on MR sialography. It is also significant that in the present study, we were able to clarify the distribution of the Bartholin and Rivinus ducts through a noninvasive analysis of the sublingual glandular ducts on MR sialography.

One possible limitation of the present study is that the number of Rivinus ducts seen on MR sialography differed from that in previous reports because of the visualization capacity. A possible explanation for this is that the sublingual ducts might have very low rate of secretion, resulting in an insufficient amount of saliva in many ducts for visualization by MR sialography. It is only natural that every image has a limit to its delineation, and clinical applications understand this limit. It is not surprising that MR sialography cannot visualize all Rivinus ducts; this will be the basis for future research. Of course, it is worthwhile to increase the accuracy of the technique with respect to improved visualization. Furthermore, we would like to improve the sequence and technique of MR sialography to improve its resulting images. Other limitations include the small sample size, imbalanced age ratio (patients with ranula were younger than subjects without sublingual gland-related disease), and the imbalanced sex ratio, as only three of the 15 patients were men. Neither sex nor race was analyzed in the study sample. In addition, differences in the distribution and patterns between sublingual and plunging ranulas were not studied; therefore, further investigation is required. Another limitation of this study is that it did not compare the results with those of X-ray sialography, 3D- cone beam computerized tomography (CBCT) sialography, or ultrasonography, which use contrast media (16,17). These imaging modalities are more invasive and difficult from an ethical standpoint because of the use of contrast media and X-rays. Further comparisons with future patient evaluations may yield new findings.

Conclusions

The results of the present study suggest that the distribution of the sublingual gland ducts, mainly, the Bartholin duct may be related to ranula formation. In addition,

various types of distributions and drainage patterns of the sublingual gland ducts were observed. These findings suggest that MR sialography of the sublingual grand ducts should be clinically applied for patients with oral diseases before undergoing a surgical procedure.

Acknowledgments

Funding: None.

Footnote

Reporting Checklist: The authors have completed the STROBE reporting checklist. Available at <https://qims.amegroups.com/article/view/10.21037/qims-23-948/rc>

Conflicts of Interest: All authors have completed the ICMJE uniform disclosure form (available at <https://qims.amegroups.com/article/view/10.21037/qims-23-948/coif>). The authors have no conflicts of interest to declare.

Ethical Statement: The authors are accountable for all aspects of the work in ensuring that questions related to the accuracy or integrity of any part of the work are appropriately investigated and resolved. The study was conducted in accordance with the Declaration of Helsinki (as revised in 2013). The study was approved by the institutional review board of Kyushu Dental University (No. 20-27). For the MRI examinations, informed consent was obtained from all patients or their parents/legal guardians. Individual consent for this retrospective analysis was waived.

Open Access Statement: This is an Open Access article distributed in accordance with the Creative Commons Attribution-NonCommercial-NoDerivs 4.0 International License (CC BY-NC-ND 4.0), which permits the non-commercial replication and distribution of the article with the strict proviso that no changes or edits are made and the original work is properly cited (including links to both the formal publication through the relevant DOI and the license). See: <https://creativecommons.org/licenses/by-nc-nd/4.0/>.

References

1. Nanci A. Ten Cate's Oral Histology: Development, Structure, and Function. 8th edition. St. Louis, MO: Mosby; 2013;255-75.
2. Harold E. Clinical Anatomy. 11th edition. Hoboken, NJ,

- USA: Blackwell Publishing; 2018;276-77.
3. Som PM, Curtin HD. Head and neck imaging. 4th edition. St. Louis, MO: Mosby; 1996:2010-1.
 4. Neri E, Boraschi P, Braccini G, Caramella D, Perri G, Bartolozzi C. MR virtual endoscopy of the pancreaticobiliary tract. *Magn Reson Imaging* 1999;17:59-67.
 5. Tanaka T, Oda M, Wakasugi-Sato N, Joujima T, Miyamura Y, Habu M, Kodama M, Takahashi O, Sago T, Matsumoto-Takeda S, Nishida I, Tsurushima H, Otani Y, Yoshiga D, Sasaguri M, Morimoto Y. First Report of Sublingual Gland Ducts: Visualization by Dynamic MR Sialography and Its Clinical Application. *J Clin Med* 2020;9:3676.
 6. Morimoto Y, Habu M, Tomoyose T, Ono K, Tanaka T, Yoshioka I, Tominaga K, Yamashita Y, Ansai T, Kito S, Okabe S, Takahashi T, Takehara T, Fukuda J, Inenaga K, Ohba T. Dynamic magnetic resonance sialography as a new diagnostic technique for patients with Sjögren's syndrome. *Oral Dis* 2006;12:408-14.
 7. Tanaka T, Ono K, Ansai T, Yoshioka I, Habu M, Tomoyose T, Yamashita Y, Nishida I, Oda M, Kuroiwa H, Wakasugi-Sato N, Okabe S, Kito S, Takahashi T, Tominaga K, Inenaga K, Morimoto Y. Dynamic magnetic resonance sialography for patients with xerostomia. *Oral Surg Oral Med Oral Pathol Oral Radiol Endod* 2008;106:115-23.
 8. Habu M, Tanaka T, Tomoyose T, Ono K, Ansai T, Ozaki Y, Yoshioka I, Yamashita Y, Kodama M, Yamamoto N, Oda M, Wakasugi N, Matsumoto S, Takahashi T, Inenaga K, Tominaga K, Morimoto Y. Significance of dynamic magnetic resonance sialography in prognostic evaluation of saline solution irrigation of the parotid gland for the treatment of xerostomia. *J Oral Maxillofac Surg* 2010;68:768-76.
 9. Tanaka T, Ono K, Habu M, Inoue H, Tominaga K, Okabe S, Kito S, Yokota M, Fukuda J, Inenaga K, Morimoto Y. Functional evaluations of the parotid and submandibular glands using dynamic magnetic resonance sialography. *Dentomaxillofac Radiol* 2007;36:218-23.
 10. Mun SJ, Choi HG, Kim H, Park JH, Jung YH, Sung MW, Kim KH. Ductal variation of the sublingual gland: a predisposing factor for ranula formation. *Head Neck* 2014;36:540-4.
 11. Leppi TJ. Gross anatomical relationships between primate submandibular and sublingual salivary glands. *J Dent Res* 1967;46:359-65.
 12. McGurk M, Eyeson J, Thomas B, Harrison JD. Conservative treatment of oral ranula by excision with minimal excision of the sublingual gland: histological support for a traumatic etiology. *J Oral Maxillofac Surg* 2008;66:2050-7.
 13. Oda M, Tanaka T, Habu M, Ono K, Kodama M, Kokuryo S, Yamamoto N, Kito S, Wakasugi-Sato N, Matsumoto-Takeda S, Nishimura S, Murakami K, Koga M, Kanuji T, Yoshiga D, Miyamoto I, Yamashita Y, Seta Y, Awano S, Yoshioka I, Matsuo K, Tominaga K, Ansai T, Inenaga K, Morimoto Y. Diagnosis and prognostic evaluation for xerostomia using dynamic MR sialography. *Curr Med Imaging Rev* 2014;10:84-94.
 14. Zhang L, Xu H, Cai ZG, Mao C, Wang Y, Peng X, Zhu ZH, Yu GY. Clinical and anatomic study on the ducts of the submandibular and sublingual glands. *J Oral Maxillofac Surg* 2010;68:606-10.
 15. Harrison JD. Modern management and pathophysiology of ranula: literature review. *Head Neck* 2010;32:1310-20.
 16. Cetinkaya V, Bonnet R, Le Thuaut A, Corre P, Mourrain-Langlois E, Delemazure-Chesneau AS, Bertin H. A comparative study of three-dimensional cone beam computed tomographic sialography and ultrasonography in the detection of non-tumoral salivary duct diseases. *Dentomaxillofac Radiol* 2023;52:20220371.
 17. Bertin H, Bonnet R, Delemazure AS, Mourrain-Langlois E, Mercier J, Corre P. Three-dimensional cone-beam CT sialography in non tumour salivary pathologies: procedure and results. *Dentomaxillofac Radiol* 2017;46:20150431.

Cite this article as: Wakasugi-Sato N, Tanaka T, Oda M, Matsumoto-Takeda S, Habu M, Nishimura S, Takahashi O, Nishida I, Tsurushima H, Otani T, Tanaka J, Nishina S, Yoshiga D, Sasaguri M, Morimoto Y. Comparison of the distribution of the Bartholin and/or Rivinus salivary ducts assessed with magnetic resonance-sialography in patients with ranula and in healthy subjects. *Quant Imaging Med Surg* 2024;14(1):397-407. doi: 10.21037/qims-23-948